Article

Petal-like CoMoO$_4$ Clusters Grown on Carbon Cloth as a Binder-Free Electrode for Supercapacitor Application

Chuanhong Chen, Hangchun Deng, Chongshi Wang, Wenqing Luo, Dejuan Huang,* and Tianxiang Jin*

ACCESS | Metrics & More | Article Recommendations

ABSTRACT: The development of supercapacitors with a high energy density and power density is of great importance for the promotion of energy storage technology. In this study, we designed and prepared petal-like CoMoO$_4$ clusters combined with carbon cloth as an excellent self-standing and binder-free electrode for asymmetric supercapacitors. Due to the abundant electrochemical active sites, the promising electron conduction, and ion diffusion rate, the CoMoO$_4$@carbon cloth (CoMoO$_4$@CC) electrode exhibits an excellent electrochemical performance. The results show that the CoMoO$_4$@CC material exhibits a high specific capacitance (664 F/g at a current density of 1 A/g) and an excellent cycle stability (capacitance remains at 84.0% after 1000 cycles). The assembled symmetrical supercapacitor has an energy density of 27 Wh/kg when the power density is 600 W/kg. Even at a higher power density (6022 W/kg), it still maintains a good energy density (18.4 Wh/kg).
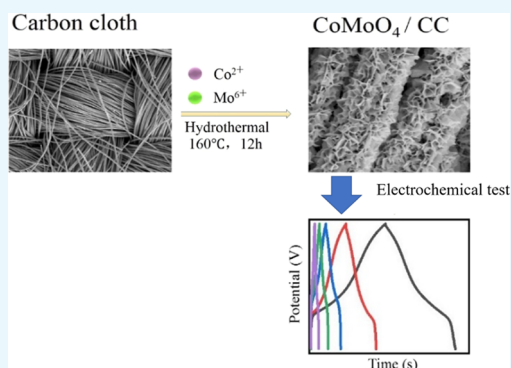
1. INTRODUCTION

With the rapid development of the society, energy consumption and environmental pollution are increasing. The use of clean energy and renewable energy has become indispensable. The development of high-power, high-capacity alternative energy conversion/storage devices, especially environmentally friendly energy conversion/storage devices, has a special significance.[1−3] Supercapacitors (SCs) are considered to be one of the most prominent and most efficient energy storage devices due to their high power density, environmental friendliness, fast charge and discharge capability, and long cycle life.[4−9]

In terms of the materials of electrodes, binary metal oxides (BTMOs) possess high electrochemical activity and have been widely studied to be promising electrode materials for energy storage devices.[10,11] Especially, metal molybdates, which are AMoO$_4$-type compounds (where A is a divalent metal ion), have potential applications in many fields such as magnetism, photoluminescence, and catalysts.[12,13] With the advantages of the high redox activity, environmental friendliness, low cost, and abundant sources, metal molybdates, such as NiMoO$_4$,[14,15] CoMoO$_4$,[16,17] and ZnCo$_2$O$_4$[18,19] have attracted more and more attention.

In the traditional SC manufacturing process, the active material is often combined with a current collector through the use of a polymer binder, which creates a "dead mass" in the active material, leading to a poor specific capacitance.[20] Moreover, most reported composite electrodes are usually made by the conventional slurry coating technology, in which the binder involved undoubtedly increases the internal resistance of the electrode. To solve these problems, many researchers grew electrochemically active substances directly on the substrate to prepare binder-free electrodes.[21,22]

In this work, we have developed a simple and effective method to prepare a CoMoO$_4$@CC material with a petal-like microstructure. CoMoO$_4$ is directly grown on carbon cloth to form a self-standing and binder-free electrode. The results prove that the CoMoO$_4$@CC electrode has a high specific capacity of 664 F/g at a current density of 1 A/g, and the capacitance retention rate exceeds 84% after 1000 cycles at a current density of 10 A/g. A symmetrical supercapacitor based on the CoMoO$_4$@CC material was assembled and tested for electrochemical performance. The symmetrical supercapacitor has a remarkable energy density of 27 Wh/kg when the power density is 600 W/kg.
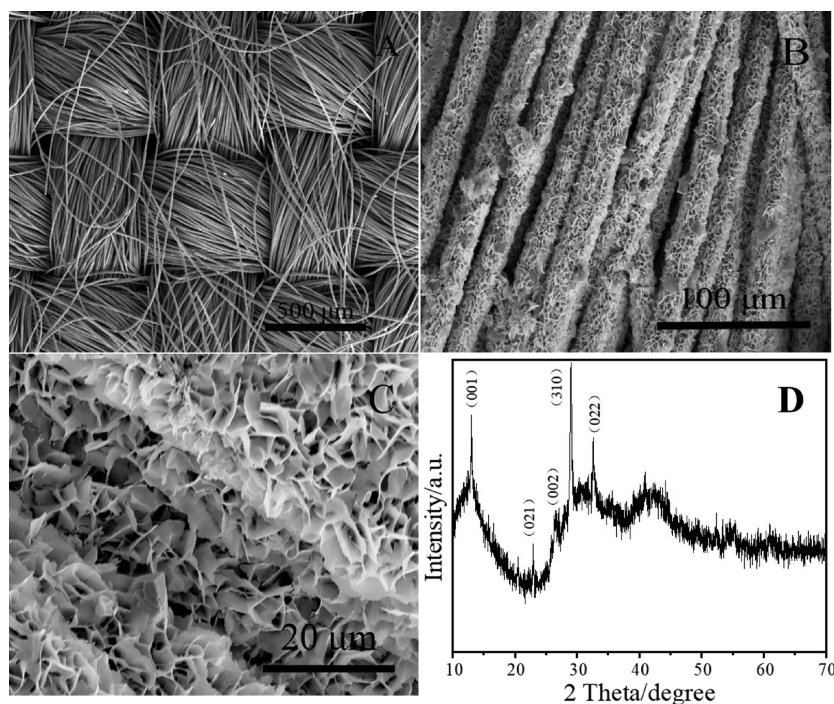
2. RESULTS AND DISCUSSION

2.1. Materials Characterization. The morphology and nanostructure of the CoMoO$_4$@CC material were studied by
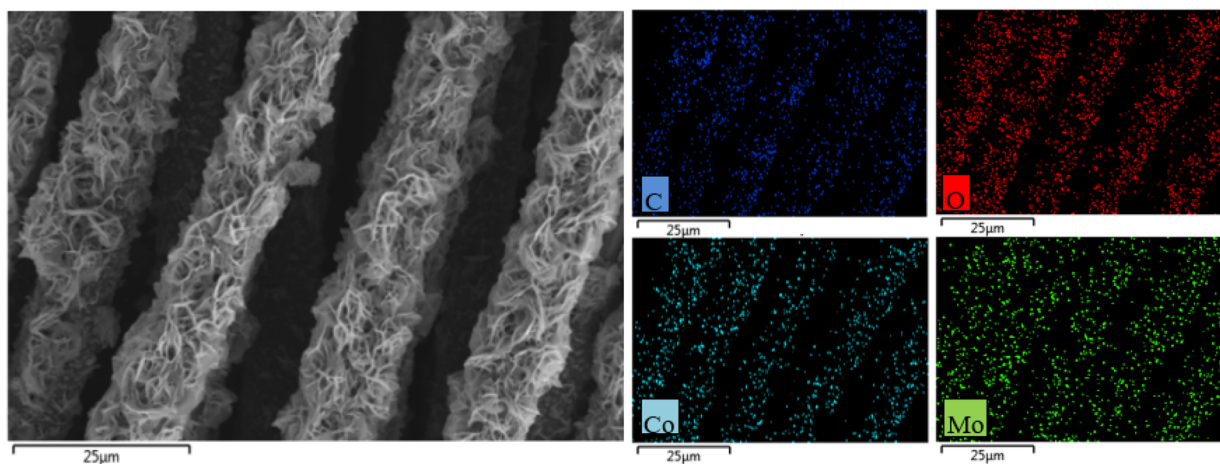
Figure 1. SEM images: (A) bare CC, (B) CoMoO$_4$@CC material, and (C) CoMoO$_4$@CC material enlarged view; (D) CoMoO$_4$@CC XRD image.


Figure 2. SEM image of CoMoO$_4$@CC and the corresponding element mapping for C, O, Co, and Mo.

scanning electron microscopy (SEM) and powder X-ray diffraction (XRD). As shown in Figure 1A, the surface morphology of the carbon cloth fiber is smooth before growth. Figure 1B,C shows the morphologies of CoMoO$_4$@CC materials under different magnifications. From the low-magnification image (Figure 1B), it can be seen that the carbon fibers are still woven together after growing CoMoO$_4$ nanosheets, and each carbon fiber is evenly covered by CoMoO$_4$ nanoflakes. Further observations show that there are a large number of densely undulating, highly ordered nanosheets on the surface of the carbon cloth. These nanosheets grow vertically to the fiber surface and are cross-linked (Figure 1C) to form a petal-like 3D nanoarray structure. This petal-like structure has a large specific surface area, which is beneficial to improve the ion diffusion rate. Moreover, this structure can also provide abundant active sites, which is beneficial to increase the specific capacitance. Figure 1D shows

the XRD result of CoMoO$_4$. Cobalt molybdate has two crystal forms (α and β forms). α-CoMoO$_4$ can transform to β-CoMoO$_4$ when the temperature is between 330 and 410 °C.[23] In this work, the CoMoO$_4$ synthesized by a hydrothermal method has an α form. In the subsequent annealing process, a part of α-CoMoO$_4$ transforms to β-CoMoO$_4$. According to XRD data, α-CoMoO$_4$ may not transform completely due to the low annealing temperature and short annealing time. The peak at $2\theta = 33.0°$ in the XRD patterns of CoMoO$_4$ is attributed to α-CoMoO$_4$ (JCPDS card number 25-1434). The diffraction peak at $2\theta = 26.4°$ corresponds to the reflection of the (002) plane of β-CoMoO$_4$ (JCPDS card number 21-0868).[24] The spectrum of CoMoO$_4$ shows wide and weak diffraction peaks, indicating that the obtained CoMoO$_4$ sample has low crystallinity. As previously reported in the literature, the poor crystallizability of the material plays a vital role in
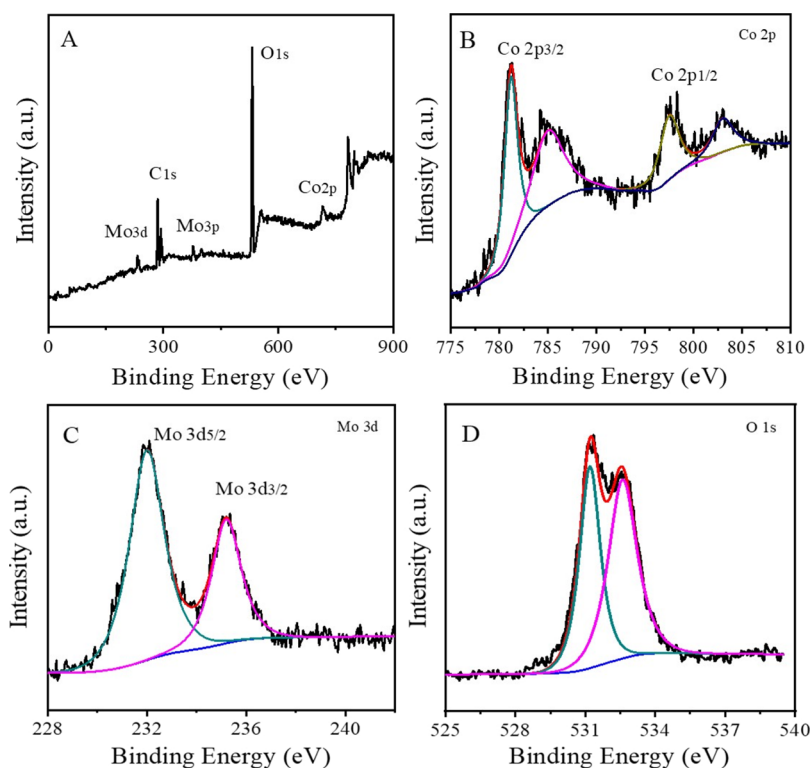
Figure 3. XPS spectrum of CoMoO₄@CC: (A) XPS full spectrum; high-resolution XPS spectrum: (B) Co 2p, (C) Mo 3d, and (D) O 1s.
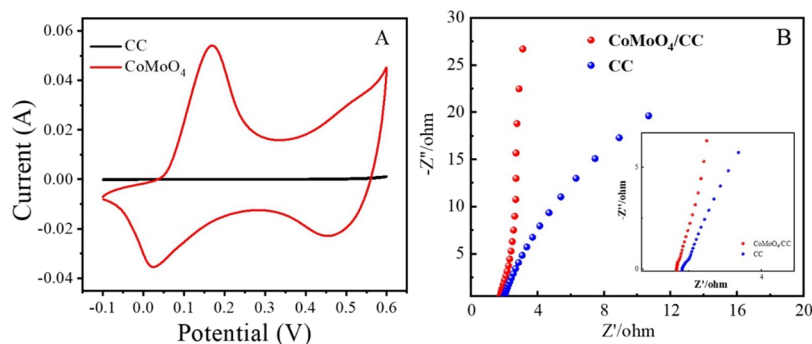
Figure 4. (A) CV curve of bare carbon cloth and CoMoO₄@CC electrode at a scan rate of 20 mV/s and (B) Nyquist plots of bare carbon cloth and CoMoO₄@CC material (the illustration is a partially enlarged Nyquist plot).

improving the electrochemical performance of supercapacitors.[25]

The X-ray energy spectrum (EDX) mapping of the SEM spectrum (Figure 2) further confirmed that CoMoO₄@CC is mainly composed of Co, Mo, C, and O elements, which are uniformly distributed throughout the carbon cloth nanowire structure. The above results confirm that CoMoO₄ is uniformly grown and covered on the carbon cloth surface.

To research the chemical composition and valence state of CoMoO₄@CC, XPS analysis was performed. As shown in Figure 3A, C, O, Mo, and Co elements were detected in the XPS spectrum. The Co 2p spectrum in Figure 3B shows two main peaks, which are the characteristic peaks of Co^{2+} in CoMoO₄@CC. The binding energy of Co 2p3/2 is 781.3 eV and the binding energy of Co 2p1/2 is 797.1 eV, indicating the oxidation state of Co^{2+}.[26,27] Figure 3C shows the Mo 3d spectrum; the peaks are located at 231.7 and 234.8 eV, which belong to Mo 3d5/2 and Mo 3d3/2, respectively. They are also the characteristic peaks of Mo^{6+} in CoMoO₄@CC,

indicating the oxidation state of Mo^{6+}.[28,29] Figure 3D shows the XPS spectrum of O 1s. The peaks at 532.5 and 531.2 eV correspond to metal−oxygen bonds and oxygen defects, respectively.[29] These results indicate that CoMoO₄@CC has been successfully prepared, which is consistent with the results of XRD and SEM-EDS.

2.2. Electrochemical Performance. A standard three-electrode system was used to conduct electrochemical tests on carbon cloth and CoMoO₄@CC electrode materials in 3 M KOH solution. Figure 4A shows the cyclic voltammetry (CV) curve of bare carbon cloth and CoMoO₄@CC electrode at a scan rate of 20 mV/s. Obviously, the current density and the surrounding area of pure CC are much lower than those of the CoMoO₄@CC electrode, which indicates that the capacitance of carbon cloth is almost negligible. For the CV curve of the CoMoO₄@CC electrode, it can be seen that there are obvious redox peaks in the range of −0.1 to 0.6 V. The redox peak originates from the faradic reaction related to the OH⁻ ion-mediated Co^{2+}/Co^{3+} ion pair in the alkaline electrolyte,
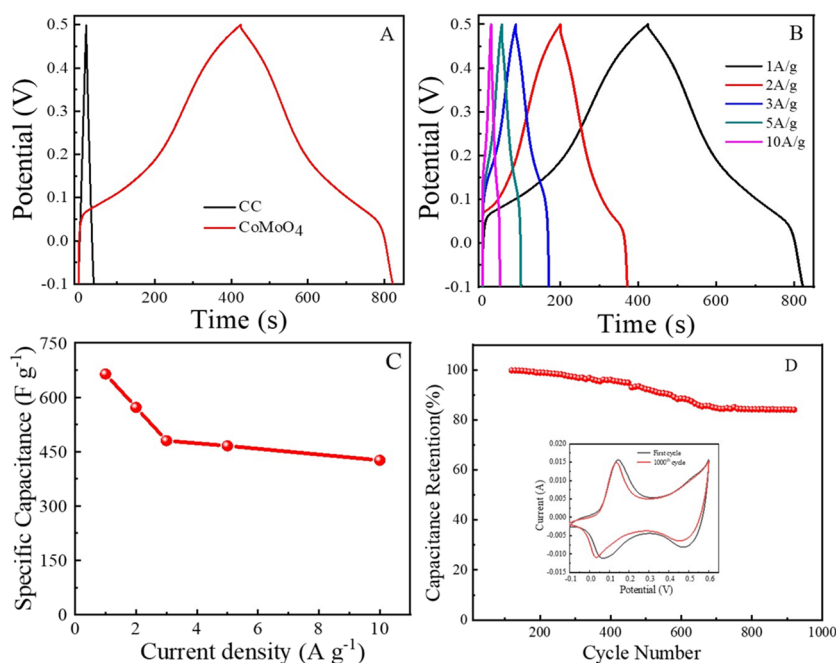
Figure 5. (A) GCD curves of CC and $CoMoO_4@CC$ materials at 1 A/g current density, (B) GCD curves of the $CoMoO_4@CC$ electrode at different current densities, (C) specific capacitance at different current densities, and (D) cycle performance test at a current density of 10 A/g.

suggesting that its capacitance is provided by the faradic redox reaction.[30]

To further understand the charge and ion transfer mechanism of this material, electrochemical impedance spectroscopy (EIS) was used. The Nyquist curves of bare carbon cloth and $CoMoO_4@CC$ electrode material are shown in Figure 4B. In the high-frequency region, the diameter of the semicircle represents the charge transfer resistance (R_{ct}), and the real-axis intercept represents the equivalent series resistance (ESR).[31] Both carbon cloth and $CoMoO_4@CC$ electrode materials show an inconspicuous semicircle and a small real-axis intercept, which means that the charge transfer resistance and equivalent series resistance are low. It can be seen from the illustration that the x-axis intercept of the $CoMoO_4@CC$ electrode material is smaller than that of bare carbon cloth, which indicates the higher electron conductivity of the $CoMoO_4@CC$ electrode. In the low-frequency region, the linear slope of the $CoMoO_4@CC$ electrode is closer to the y axis than that of the carbon cloth electrode, which indicates that the electrode has a faster ion diffusion rate. These excellent properties can be ascribed to the petal-like structure of the $CoMoO_4$ clusters. This structure can increase the contact area between the electrolyte and the active material, shorten the ion transport channel, and improve the charge transport efficiency.

Figure 5A displays the galvanostatic charge−discharge- (GCD) curves of carbon cloth and $CoMoO_4@CC$ electrodes at a current density of 1 A/g. Obviously, the discharge time of bare CC is much shorter than that of $CoMoO_4@CC$ electrode, which indicates that the specific capacitance of pure CC is almost negligible. This result is consistent with its CV test results. Figure 5B shows the GCD curves of the $CoMoO_4@CC$ electrode at current densities ranging from 1 to 10 A/g. The GCD curves at all current densities are nonlinear and well symmetrical, indicating that most of the capacitance of this material is pseudocapacitance. Moreover, the corresponding Coulomb efficiency of $CoMoO_4@CC$ can reach 96.7%,

indicating excellent reversibility. The specific capacitance values are calculated according to the discharge curve, and the results are shown in Figure 5C. The value of Cs decreases with the increase in the current density. This is because less ions can reach the electrode surface as the current density increases.[32] When the current densities are 1, 2, 3, 5, and 10 A/g, the specific capacitances of $CoMoO_4@CC$ are 664, 572, 480, 466, and 426 F/g, respectively. Even if the current density is increased by 10 times, it can still maintain a high specific capacitance. Figure 5D shows the results of the cycle stability test at a current density of 10 A/g. The capacity retention rate can reach 84% after 1000 cycles. The sharp decrease in the specific capacitance in the initial 400 charge/discharge cycles can be explain as the presence of the electrochemically active but unstable oxygen groups.[33] The illustration in Figure 5D shows the comparison of the CV curve between the first cycle and the 1000th cycle. It can be seen that the CV curve is almost unchanged after 1000 cycles. These data indicate that the $CoMoO_4@CC$ material has an excellent cyclic stability.

To evaluate the energy storage capacity of $CoMoO_4@CC$, the electrochemical performance of this work was compared with that of several previous reports about Mo-based electrodes. As can be seen in Table 1, the $CoMoO_4@CC$ electrode showed a competitive electrochemical performance, which means that $CoMoO_4@CC$ is an ideal electrode material for supercapacitors.

2.3. Symmetrical Supercapacitor Performance Test. To further investigate the actual performance of $CoMoO_4@$ CC, we assembled a symmetrical supercapacitor with two identical $CoMoO_4@CC$ electrodes. Figure 6A shows the CV curve of the $CoMoO_4@CC\|CoMoO_4@CC$ supercapacitor at a scan rate of 10 mV/s in different voltage windows. The supercapacitor shows a typical quasi-rectangular CV curve in the voltage range of 0−1.2 V, which indicates that it has good cycle reversibility in a broad voltage window of 0−1.2 V. The GCD curves of the $CoMoO_4@CC\|CoMoO_4@CC$ super-capacitor are shown in Figure 6B. The shape of the GCD

Table 1. Comparison Data of the Performance of the CoMoO4@CC Electrode Material with References

electrode material	current density	specific capacitance	capacity retention	cycle number
MoS$_2$/C[34]	0.2 A g^{-1}	201 F g^{-1}	94.1%	1000
MoO$_3$/Ag[35]	1 A g^{-1}	225 F g^{-1}	71.1%	10,000
α-MoO$_3$[36]	5 mV s^{-1}	30 F g^{-1}	80%	100
α-MoO$_3$[37]	0.6 mA cm^{-1}	73.6 F g^{-1}	94.7%	2000
CoMoO$_4$/chitosan[38]	2 mA cm^{-2}	71 F g^{-1}	81%	2000
CoMoO$_4$/C[39]	1 A g^{-1}	109.4 F g^{-1}	99.8%	200
CoMoO$_4$@CC (this work)	1 A g^{-1}	664 F g^{-1}	84%	1000

curves is similar to an isosceles triangle, confirming that the device has good reversibility in the entire potential range.

According to the discharge time and total mass of the electrode materials, the specific capacitance at different current densities is calculated and recorded in Figure 6C. At a current density of 1 A/g, the specific capacitance of the device is 67.5 F/g. When the current density is increased to 10 A/g, the capacitance is 46 F/g, which retains 68.1% of its initial value. Figure 6D shows the Ragone plot of the supercapacitor of this work and other Mo-based supercapacitors. It is worth noting that the maximum energy density of the CoMoO$_4$@CC‖CoMoO$_4$@CC device can reach 27 Wh/kg when the power density is 600 W/kg, superior to those of other reported materials for supercapacitors, for instance, MoO$_3$/Ag (15.51 Wh/kg, 348.97 W/kg),[34] microrod-architectured MoO$_3$ (7.33 Wh/kg, 1200 W/kg),[40] MoS$_2$/MoO$_3$/PPy (10 Wh/kg, 203 W/kg),[41] NiMoO$_4$ (20.1 Wh/kg, 2100 W/kg), and MoO$_3$/PPy/rGO (19.8 Wh/kg, 301 W/kg).[14,42] Even at a high

current density of 10 A/g, its energy density is still maintained at 18.4 Wh/kg. All these excellent results prove that CoMoO$_4$@CC‖CoMoO$_4$@CC has a bright future in the application of supercapacitors.

3. EXPERIMENTAL SECTION

3.1. Chemicals. Ammonium molybdate ((NH$_4$)$_6$Mo$_7$O$_{24}$·4H$_2$O, AR), cobalt chloride (CoCl$_2$·6H$_2$O), nitric acid (HNO$_3$, 65%), sulfuric acid (H$_2$SO$_4$, AR), and polyvinylpyrrolidone (PVP, AR grade) were purchased from Aladdin Co., Ltd. (China). Urea (CO(NH$_2$)$_2$) and ethanol (C$_2$H$_5$OH) were purchased from Sinopharm Reagent. Potassium hydroxide (KOH) was purchased from Xilong Science, and carbon cloth (CC) was purchased from Suzhou Yilongsheng Energy Technology Co., Ltd. Deionized (DI) water was used throughout the experiment. All reagents are analytically pure and no further purification is required.

3.2. Experimental Steps. *3.2.1. Experimental Plan Design.* Using CoCl$_2$·6H$_2$O and (NH$_4$)$_6$Mo$_7$O$_{24}$ as raw materials and carbon cloth as the substrate, the CoMoO$_4$@CC material was synthesized through the hydrothermal reaction and annealing process.

3.2.2. Carbon Cloth Pretreatment. A mixed solution of 10% nitric acid and 10% sulfuric acid (3 nitrate:1 sulfur) was used to pretreat the carbon cloth at 120 °C for 3 h to improve the hydrophilicity. Then, it was washed with acetone, ethanol, and deionized water ultrasonically for 30 min to remove the grease and dirt on the surface. Finally, it was vacuum-dried at 60 °C for 12 h.

3.2.3. Preparation of CoMoO$_4$@CC. Dissolve 720 mg of CoCl$_2$·6H$_2$O, 520 mg of (NH$_4$)$_6$Mo$_7$O$_{24}$, 480 mg of CO-(NH$_2$)$_2$, and 100 mg of PVP in 40 mL of deionized water.
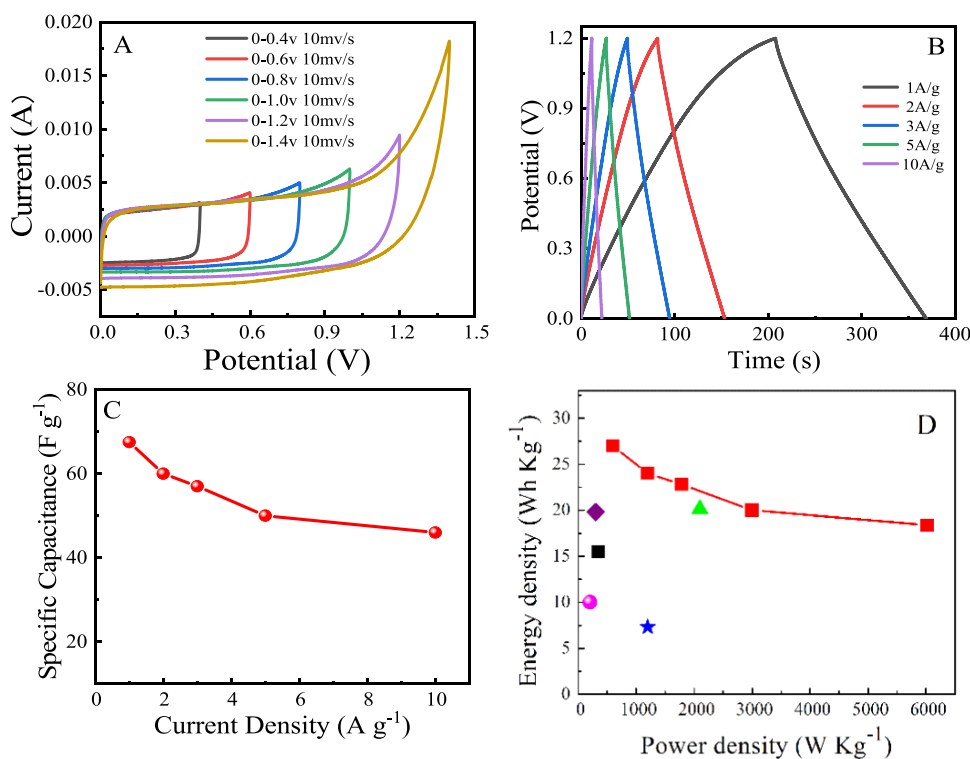
Figure 6. Electrochemical performance of the CoMoO$_4$@CC‖CoMoO$_4$@CC symmetrical supercapacitor in 1 M Na$_2$SO$_4$ neutral electrolyte: (A) CV curves of different voltage ranges when the sweep speed is 10 mV/s; (B) GCD curves at various current densities; (C) specific capacitance under different current densities; (D) Ragone curve diagram.

After stirring for 20 min, the solution was transferred to a 100 mL autoclave and the pretreated carbon cloth (2×2 cm) was added to the kettle, then sealed, and hydrothermally reacted at 160 °C for 12 h. After the autoclave was cooled to room temperature, the samples were collected, washed several times with water and ethanol, and dried at 60 °C. Finally, the $CoMoO_4$@CC sample was heated to 350 °C at a heating rate of 5 °C min^{-1} and annealed in a N_2 environment for 3 h.

3.3. Materials Characterization. Field emission scanning electron microscopy (FESEM) was performed on a Nova Nano SEM 450 scanning electron microscope. The XPS measurement was performed on a Thermo Fisher X-ray photoelectron spectrometer equipped with Al radiation as a probe ($K\alpha$, radiation), the chamber pressure was 5×10^{-9} Torr, and the diameter of the analysis spot was 400 μm. The crystal structure of the sample was studied by XRD (D8 Advance, Germany).

3.4. Electrochemical Tests. Whole electrochemical tests were carried out on a CHI660E workstation (Shanghai Chenhua) in 3 M KOH aqueous solution. A three-electrode system was used to investigate the electrochemical performance of the samples. A saturated calomel electrode and Pt wire served as the reference and counter electrodes, respectively.

A two-electrode system was used to study the electrochemical properties of the symmetric supercapacitor constructed by assembling two similar $CoMoO_4$@CC electrodes. The specific capacitances (Cs) of the individual electrode and the two-electrode cell were calculated from the galvanostatic discharge curves by eq 1. The specific energy density (Ec) and specific power density (Pc) were calculated according to eqs 2 and 3, respectively:

$$Cs = \frac{I\Delta t}{m\Delta U} \tag{1}$$

$$Ec = \frac{Cs\Delta U^2}{2 \times 3.6} \tag{2}$$

$$Pc = \frac{Ec \times 3600}{\Delta t} \tag{3}$$

where I is the discharge current, Δt is the discharge time, m is the mass of the active material in a three-electrode system in a two-electrode cell, m is the total active mass of both electrodes, and ΔU is the voltage window.

4. CONCLUSIONS

In this work, the petal-like $CoMoO_4$ clusters have been directly synthesized on the carbon cloth substrate by a simple hydrothermal method. Electrochemical studies show that the $CoMoO_4$@CC electrode material has an excellent pseudocapacitance performance. The $CoMoO_4$@CC material displays a high specific capacitance (664 F/g at a current density of 1A/g) and an excellent cycle stability (capacitance remains at 84% after 1000 cycles). The assembled symmetrical supercapacitor has an energy density of 27 Wh/kg when the power density is 600 W/kg. Moreover, the energy density can still remain at 18.4 Wh/kg at a high power density of 6022 W/kg. This convenient method provides an effective way to enhance the electrochemical performance of supercapacitors and shows broad application prospects in future energy storage systems.

■ AUTHOR INFORMATION

Corresponding Authors

Dejuan Huang − *School of Chemistry, Biology, and Materials Science, East China University of Technology, Nanchang 330013 Jiangxi, China*; Email: djhuang@ecut.edu.cn

Tianxiang Jin − *School of Chemistry, Biology, and Materials Science, East China University of Technology, Nanchang 330013 Jiangxi, China;* ◉ orcid.org/0000-0001-5950-6792; Email: 201660027@ecut.edu.cn

Authors

Chuanhong Chen − *School of Chemistry, Biology, and Materials Science, East China University of Technology, Nanchang 330013 Jiangxi, China*

Hangchun Deng − *School of Chemistry, Biology, and Materials Science, East China University of Technology, Nanchang 330013 Jiangxi, China*

Chongshi Wang − *College of Engineering, Department of Civil, Architectural & Environmental Engineering, Drexel University, Philadelphia, Pennsylvania 19104, United States*

Wenqing Luo − *School of Chemistry, Biology, and Materials Science, East China University of Technology, Nanchang 330013 Jiangxi, China*

Complete contact information is available at:
https://pubs.acs.org/10.1021/acsomega.1c02166

Notes

The authors declare no competing financial interest.

■ REFERENCES

(1) Zhu, M.; Shao, Q.; Pi, Y.; Guo, J.; Huang, B.; Qian, Y.; Huang, X. Ultrathin Vein-Like Iridium−Tin Nanowires with Abundant Oxidized Tin as High-Performance Ethanol Oxidation Electrocatalysts. *Small* **2017**, *13* (36), 1701295.

(2) Zhu, M.; Shao, Q.; Qian, Y.; Huang, X. Superior Overall Water Splitting Electrocatalysis in Acidic Conditions Enabled by Bimetallic Ir-Ag Nanotubes. *Nano Energy* **2019**, *56*, 330−337.

(3) Zhu, T.; Ding, J.; Shao, Q.; Qian, Y.; Huang, X. ,Se-Codoped MoS2 Nanosheets as Accelerated Electrocatalysts for Hydrogen Evolution. *ChemCatChem* **2019**, *11* (2), 689−692.

(4) Chen, J.; Lin, C.; Zhang, M.; Jin, T.; Qian, Y. Constructing Nitrogen, Selenium Co-Doped Graphene Aerogel Electrode Materials for Synergistically Enhanced Capacitive Performance. *ChemElectroChem* **2020**, *7* (15), 3311−3318.

(5) Yang, L.; Lu, X.; Wang, S.; Wang, J.; Guan, X.; Guan, X.; Wang, G. Designed synthesis of nickel−cobalt-based electrode materials for high-performance solid-state hybrid supercapacitors. *Nanoscale* **2020**, *12*, 1921−1938.

(6) Gao, M.; Wang, W.-K.; Rong, Q.; Jiang, J.; Zhang, Y.-J.; Yu, H.-Q. Porous ZnO-coated Co_3O_4 nanorod as a high-energy-density supercapacitor material. *ACS Appl. Mater. Inter.* **2018**, *10*, 23163−23173.

(7) Qu, G.; Sun, P.; Xiang, G.; Yin, J.; Wei, Q.; Wang, C.; Xu, X. Moss-like nickel-cobalt phosphide nanostructures for highly flexible all-solid-state hybrid supercapacitors with excellent electrochemical performances. *Appl. Mater. Today* **2020**, *20*, 100713.

(8) Yang, L.; Yang, Y.; Wang, S.; Guan, X.; Guan, X.; Wang, G. Multi-Heteroatom-Doped Carbon Materials for Solid-State Hybrid

Supercapacitors with a Superhigh Cycling Performance. *Energy Fuels* **2020**, *34*, 5032−5043.

(9) Wang, J.; Yang, L.; Fu, Y.; Yin, P.; Guan, X.; Wang, G. Delicate control of crystallographic Cu2O derived Ni−Co amorphous double hydroxide nanocages for high-performance hybrid supercapacitors: an experimental and computational investigation. *Nanoscale* **2021**, *13*, 8562−8574.

(10) Fu, W.; Wang, Y.; Han, W.; Zhang, Z.; Zha, H.; Xie, E. Construction of hierarchical ZnCo$_2$O$_4$ @ Ni$_x$Co$_{2x}$ (OH)$_{6x}$ core/shell nanowire arrays for high-performance supercapacitors. *J. Mater. Chem. A* **2016**, *4*, 173−182.

(11) Zhou, M.; Lu, F.; Shen, X.; Xia, W.; He, H.; Zeng, X. One-pot construction of three dimensional CoMoO$_4$/Co$_3$O$_4$ hybrid nanostructures and their application in supercapacitors. *J. Mater. Chem. A* **2015**, *3*, 21201−21210.

(12) Hall, P. J.; Mirzaeian, M.; Fletcher, S.; Sillars, F. B.; Rennie, A. J. R.; Shitta-Bey, G. O.; Wilson, G.; Cruden, A.; Carter, R. Energy storage in electrochemical capacitors: designing functional materials to improve performance. *Energy Environ. Sci.* **2010**, *3*, 1238−1251.

(13) Rodriguez, J.; Chaturvedi, S.; Hanson, J.; Albornoz, A.; Brito, J. L. Electronic properties and phase transformations in CoMoO$_4$ and NiMoO$_4$: XANES and time-resolved synchrotron XRD studies. *J. Phys. Chem. B* **1998**, *102*, 1347−1355.

(14) Cai, D.; Wang, D.; Liu, B.; Wang, Y.; Liu, Y.; Wang, L.; Li, H.; Huang, H.; Li, Q.; Wang, T. Comparison of the electrochemical performance of NiMoO4 nanorods and hierarchical nanospheres for supercapacitor applications. *ACS Appl. Mater. Inter.* **2013**, *5*, 12905−12910.

(15) Peng, S.; Li, L.; Wu, H. B.; Madhavi, S.; Lou, X. W. D. Controlled growth of NiMoO$_4$ nanosheet and nanorod arrays on various conductive substrates as advanced electrodes for asymmetric supercapacitors. *Adv. Energy Mater.* **2015**, *5*, 1401172.

(16) Cao, Y.; An, L.; Liao, L.; Liu, X.; Ji, T.; Zou, R.; Yang, J.; Qin, Z.; Hu, J. Hierarchical core/shell structures of ZnO nanorod@ CoMoO$_4$ nanoplates used as a high-performance electrode for supercapacitors. *RSC Adv.* **2016**, *6*, 3020−3024.

(17) Yu, X.; Lu, B.; Xu, Z. Super long-life supercapacitors based on the construction of nanohoneycomb-like strongly coupled CoMoO$_4$-3D graphene hybrid electrodes. *Adv. Mater.* **2014**, *26*, 1044−1051.

(18) Wu, H.; Lou, Z.; Yang, H.; Shen, G. A flexible spiral-type supercapacitor based on ZnCo2O4 nanorod electrodes. *Nanoscale* **2015**, *7*, 1921.

(19) Liu, B.; Liu, B.; Wang, Q.; Wang, X.; Xiang, Q.; Chen, D.; Shen, G. New energy storage option: toward ZnCo$_2$O$_4$ nanorods/nickel foam architectures for high-performance supercapacitors. *ACS Appl. Mater. Inter.* **2013**, *5*, 10011−10017.

(20) Wang, G.; Zhang, L.; Zhang, J. A review of electrode materials for electrochemical supercapacitors. *Chem. Soc. Rev.* **2012**, *41*, 797−828.

(21) Liu, J.; Jiang, J.; Cheng, C.; Li, H.; Zhang, J.; Gong, H.; Fan, H. J. Co$_3$O$_4$nanowire@ MnO$_2$ ultrathin nanosheet core/shell arrays: a new class of highperformance pseudocapacitive materials. *Adv. Mater.* **2011**, *23*, 2076−2081.

(22) Ling, J.; Zou, H.; Yang, W.; Chen, W.; Lei, K.; Chen, S. Facile fabrication of polyaniline/molybdenum trioxide/activated carbon cloth composite for supercapacitors. *J. Energy Storage* **2018**, *20*, 92−100.

(23) Rico, J. L.; Ávalos-Borja, M.; Barrera, A.; Hargreaves, J. S. J. Template-free synthesis of CoMoO4 rods and their characterization. *Mater. Res. Bull.* **2013**, *48*, 4614−4617.

(24) Xu, X.; Shen, J.; Li, N.; Ye, M. Microwave-assisted synthesis of graphene/CoMoO4 nanocomposites with enhanced supercapacitor performance. *J. Alloys Compd.* **2014**, *616*, 58−65.

(25) Liu, M.-C.; Kong, L.-B.; Kang, L.; Li, X.; Walsh, F. C.; Xing, M.; Lu, C.; Ma, X.-J.; Luo, Y. Synthesis and characterization of M$_3$V$_2$O$_8$ (M = Ni or Co) based nanostructures: a new family of high performance pseudocapacitive materials. *J. Mater. Chem. A* **2014**, *2*, 4919−4926.

(26) Nti, F.; Anang, D.; Han, J. I. Facilely synthesized NiMoO$_4$/ CoMoO$_4$ nanorods as electrode material for high performance supercapacitor. *J. Alloys Compd.* **2018**, *742*, 342−350.

(27) Li, Z.; Zhao, D.; Xu, C.; Ning, J.; Zhong, Y.; Zhang, Z.; Wang, Y.; Hu, Y. Reduced CoNi$_2$S$_4$ nanosheets with enhanced conductivity for high-performance supercapacitors. *Electrochim. Acta* **2018**, *278*, 33−41.

(28) Ghosh, D.; Giri, S.; Das, C. K. Synthesis, characterization and electrochemical performance of graphene decorated with 1D NiMoO$_4$ ·nH$_2$O nanorods. *Nanoscale* **2013**, *5*, 10428−10437.

(29) Chen, C.; Wang, S.; Luo, X.; Gao, W.; Huang, G.; Zeng, Y.; Zhu, Z. Reduced ZnCo$_2$O$_4$@NiMoO$_4$·H$_2$O heterostructure electrodes with modulating oxygen vacancies for enhanced aqueous asymmetric supercapacitors. *J. Power Sources* **2019**, *409*, 112−122.

(30) Senthilkumar, B.; Meyrick, D.; Lee, Y.-S.; Selvan, R. K. Synthesis and improved electrochemical performances of nano β-NiMoO$_4$-CoMoO$_4$·xH$_2$O composites for asymmetric supercapacitors. *RSC Adv.* **2013**, *3*, 16542−16548.

(31) Li, H.; Zhang, X.; Ding, R.; Qi, L.; Wang, H. Facile synthesis of mesoporous MnO$_2$ microspheres for high performance AC//MnO$_2$ aqueous hybrid supercapacitors. *Electrochim. Acta* **2013**, *108*, 497−505.

(32) Nasini, U.; Bairi, V.; Ramasahayam, S.; Bourdo, S.; Viswanathan, T.; Shaikh, A. U. Phosphorous and nitrogen dual heteroatom doped mesoporous carbon synthesized via microwave method for supercapacitor application. *J. Power Sources* **2014**, *250*, 257.

(33) Wang, C.; Zhou, Y.; Sun, L.; Wan, P.; Zhang, X.; Qiu, J. Sustainable synthesis of phosphorus- and nitrogen-co-doped porous carbons with tunable surface properties for supercapacitors. *J. Power Sources* **2013**, *239*, 81−88.

(34) Fan, L.-Q.; Liu, G.-J.; Zhang, C.-Y.; Wu, J.-H.; Wei, Y.-L. Facile one-step hydrothermal preparation of molybdenum disulfide/carbon composite for use in supercapacitor. *Int. J. Hydrogen Energy* **2015**, *40*, 10150−10157.

(35) Zhou, C.; Wang, Q.; Yan, X.; Wang, J. J.; Wang, D. F.; Yuan, X. X.; Jiang, H.; Zhu, Y. H.; Cheng, X. N. A facile route to synthesize Ag decorated MoO$_3$ nanocomposite for symmetric supercapacitor. *Ceram. Int.* **2020**, *46*, 15385−15391.

(36) Shakir, I.; Shahid, M.; Yang, H. W.; Kang, D. J. Structural and electrochemical characterization of α-MoO$_3$ nanorod-based electrochemical energy storage devices. *Electrochim. Acta* **2010**, *56*, 376−380.

(37) Prakash, N.; Dhananjaya, M.; Narayana, A.; Shaik, D.; Rosaiah, P.; Hussain, O. High performance one dimensional α-MoO$_3$ nanorods for supercapacitor applications. *Ceram. Int.* **2018**, *44*, 9967−9975.

(38) Ramkumar, R.; Sundaram, M. A biopolymer gel-decorated cobalt molybdate nanowafer: effective graft polymer cross-linked with an organic acid for better energy storage. *New J. Chem.* **2016**, *40*, 2863−2877.

(39) Li, J.; Zhao, C.; Yang, Y.; Li, C.; Hollenkamp, T.; Burke, N.; Hu, Z.; Tendeloo, G. V.; Chen, W. Synthesis of monodispersed CoMoO4 nanoclusters on the ordered mesoporous carbons for environment-friendly supercapacitors. *J. Alloy. Compound.* **2019**, *810*, 151841−151849.

(40) Pujari, R. B.; Lokhande, V. C.; Kumbhar, V. S.; Chodankar, N. R.; Lokhande, C. D. Hexagonal microrods architectured MoO3 thin film for supercapacitor application. *J. Mater. Sci.* **2016**, *27*, 3312.

(41) Sari, F. N. I.; Ting, J.-M. High performance asymmetric supercapacitor having novel 3D networked polypyrrole nanotube/N-doped graphene negative electrode and core-shelled MoO3/PPy supported MoS2 positive electrode. *Electrochim. Acta* **2019**, *320*, 134533.

(42) Deng, H.; Huang, J.; Hu, Z.; Chen, X.; Huang, D.; Jin, T. Fabrication of a Three-Dimensionally Networked MoO3/PPy/rGO Composite for a High-Performance Symmetric Supercapacitor. *ACS Omega* **2021**, *6*, 9426−9432.